ORIGINAL ARTICLE

The effect of the diode laser beam power on the behaviour of the ZrC powder pre-coat and the 145Cr6 steel substrate during laser processing

Dariusz Bartkowski[1] · Aneta Bartkowska[2] · Peter Jurči[3] · Martin Kusý[3] · Damian Przestacki[1] · Dariusz Ulbrich[4]

Abstract

The paper presents both the production method and its impact on selected properties of composite coatings reinforced with hard ZrC particles. The Fe/ZrC coatings were produced using diode laser by remelting the pre-coat in the form of paste consisting of ZrC powder and binder. Different values of laser beam power (500 W, 700 W, and 900 W) and different pre-coat thicknesses (100 μm, 150 μm, and 200 μm) were used to produce the composite coatings. During all processes, the scanning speed of laser beam was 3 m/min. Laser beam spot diameter was 1 mm. Microstructure study, microhardness tests, as well as EDS and XRD analysis were carried out. The obtained Fe/ZrC coatings were also tested for the effect of the corrosive medium in a 3.5% NaCl water solution. The effect of applied parameters on wear resistance of Fe/ZrC coatings was also studied. The tribological properties were assessed both by mass loss measurement and by scanning electron microscopy. Fe/ZrC coatings produced using the highest thickness of the pre-coat were characterised by cracks arising during production process. The very high concentration of carbides and hence high hardness of the coating produced in this way contributed to it. However, a positive effect of laser beam power increase on reduction of these cracks was observed. The coatings were characterised by very high hardness, reaching in some cases even more than 2000 HV. It was found that the most favourable properties regarding both tribology and corrosion resistance were obtained for Fe/ZrC coatings produced using 150 μm of pre-coat thickness.

Keywords ZrC coatings · Laser processing · Metal matrix composite coatings · Microstructure

1 Introduction

In recent years, research workers very often tackle the problem of using high-energy energy sources for material processing. Cutting metal materials with a plasma stream [1] or with a laser beam [2] has become a standard in industry. Laser welding is also very common. Processes of surface modification of materials [3, 4] or hybrid processing, which combines two or more technological processes, are also becoming more and more widespread. An example of hybrid processing can be laser-assisted turning described in papers [5], which consists in heating the surface of very hard materials immediately before the turning process, thus reducing its hardness. However, many more studies concern modification of material surfaces by weld surfacing or alloying with a laser beam. These processes involve introducing into the surface of substrate material elements and chemical compounds which improve mechanical and physicochemical properties of the surface. Here laser beam is used not to heat the material but to remelt it and permanently connect the substrate with the additional material. Research workers are trying to refine surfaces using various types of materials. Studies are known in which boron was introduced [6] into surface of steel, forming hard iron borides. Processes have

✉ Dariusz Bartkowski
dariusz.bartkowski@put.poznan.pl

1 Faculty of Mechanical Engineering, Poznan University of Technology, Ul. Piotrowo 3, 60-965 Poznań, Poland

2 Faculty of Materials Engineering and Technical Physics, Poznan University of Technology, Jana Pawła II 24, 60-965 Poznan, Poland

3 Faculty of Materials Science and Technology in Trnava, Slovak University of Technology in Bratislava, Jána Bottu 25, 917-24 Trnava, Slovakia

4 Faculty of Civil and Transport Engineering, Poznan University of Technology, Ul. Piotrowo 3, 60-965 Poznań, Poland

also been described such as refining the substrate by remelting the pre-coat containing high-melt metals and graphite [7], aiming to form carbides of these metals. Here, carbides are formed in situ in the produced coating. Laser cladding methods allow the introduction of carbide particles directly into the laser beam. The most commonly described reinforcing phase is tungsten carbides (WC). They are introduced into the steel in the form of a powder mixture, in which beside tungsten carbide particles there is also a powder acting as a matrix. The matrix materials are most frequently nickel alloys, such as NiCrBSi [8], Inconel [9], but also cobalt alloys, such as Stellite [10–12]. Research papers can also be found on powder coatings in which tungsten carbides alone were introduced without matrix powder [13]. The matrix then became the base material laser beam remelted and mixed with the reinforcing phase.

Tungsten carbide appears to be a material most commonly used by researchers in applying laser technologies in surface engineering. Therefore, it is justifiable to check the possibility of using other carbides. Researchers carry out processes of refining surface layer of materials by alloying a pre-coat containing a given compound or chemical element. As a result of laser beam impact hard phases are formed. These phenomena take place during the crystallisation of the material which is simultaneously remelted by the laser beam. The materials used for surface refinement are chemical elements with a high affinity for carbon, i.e. tungsten, chromium, vanadium, or titanium [14, 15]. These elements are part of cemented carbides.

A very interesting group of tool materials is cermets, i.e. metal-ceramic sinters. They consist of two very hard carbides: tantalum carbide (TaC) and zirconium carbide (ZrC). Preliminary tests undertaken in the studies [16, 17] justify the use of these two carbides in surface engineering processes. The author attempted to remelt the ZrC paste with a laser beam in order to obtain a composite coating. The preliminary tests described in the paper [17] focused on a single laser track, and this work is its extension by a number of material tests.

There is a fairly limited number of publications on production of composite coatings by introducing primary ZrC particles with a laser beam. For example, in the work [18], studies were undertaken to produce a composite coating constructed of a copper matrix and a reinforcing phase of ZrB_2-ZrC. Laser welding and self-propagating high-temperature synthesis (SHS) reactions were used. The ZrC phase was synthesised in situ in the coating. As a result, rectangular ZrC phases with lengths of approximately 500 nm. This allowed obtaining a coating hardness of approximately 400 HV, which significantly exceeded the hardness of the copper substrate. Synthesis in situ of the ZrC phase was also the subject of a study [19]. The researchers used laser cladding by introducing into AISI

1045 steel a mixture consisting of Ni25 powder, carbon, and ZrO_2. As a result, they obtained a ZrC phase that was evenly distributed in the composite coating. Various proportions of the powder mixture were also tested. It was found that the forming ZrC phase has a positive effect on coating hardness. A hardness of 650 HV was achieved, which was more than double the hardness of coatings produced only with Ni25 powder. ZrC powder was also used by King et al. [20] in the selective laser melting (SLM) process. Along with zirconium carbide, the powder used also contained ZrB_2 and B_4C. To the best knowledge of the authors of this paper, it was the first application of a high-temperature powder mixture in the SLM process. The coating was produced on a tungsten substrate. Very hard ZrC layers were also produced by Craciun et al. [21]. They used pulsed laser deposition technique and obtained thin ZrC layers with a hardness of approximately 40 GPa. On the other hand, Liu et al. [22] studied coatings made of ZrC as well as ZrC-SiC and ZrC-TiC. They were produced using vacuum plasma spray method. The authors checked how the produced layers react to laser ablation process and concluded that the proposed layers may be an example of a material that is ablation resistant. Bartkowski et al. [23] produced ZrC coatings on Monel-400 alloy using ZrC pre-coat remelting process. It was found that it is possible to produce a ZrC-reinforced composite coating characterised by a much higher hardness compared to the substrate. It was also found that increasing laser beam power reduces hardness of the modified coatings. Studies of coatings containing ZrC were also carried out by Zhang et al. [24], who obtained this phase in situ in laser cladding process. They used a 3-kW CO_2 laser and the initial material was a mixture of iron-based powder and zirconium powder. The reinforcing phase made it possible to produce a coating with hardness in the range of 1000–1200 HV0.2. They produced both single and multiple tracks and concluded that the amount and size of ZrC particles are higher in multiple tracks than in single tracks.

Analysing the literature available in international scientific databases, it can be concluded that there are very few publications discussing the process of introducing primary ZrC particles into the surface layer. Most commonly this phase is produced in situ in the coatings formed. Therefore, the introduction of primary ZrC particles is a novelty in surface engineering. Bartkowski's preliminary studies of individual tracks allowed for the development of manufacturing parameters that could be successfully applied in full-size coatings. It should also be noted that majority of studies on the introduction of carbides into the surface layers are based on the use of a powder mixture which contains matrix material. The method presented in this paper consists in introducing only the reinforcement phase and adapting the substrate material as a matrix. The authors have already

presented such a possibility for WC particles introduced by laser cladding into steel [13], which became an inspiration to carry out similar tests on ZrC particles.

This paper focuses on the influence of pre-coat thickness and laser beam power on the behaviour of the pre-coat and the steel substrate. The obtained coating was subjected to tests of microstructure, microhardness, wear resistance by friction, and corrosion resistance. Chemical and phase composition tests were also carried out, at the same time trying to explain the reasons for obtaining individual properties.

2 Research methodology

2.1 Materials

Fe/ZrC metal matrix composite coatings were produced on 145Cr6 low alloy tool steel. The dimension of specimens was $20 \times 20 \times 8$ mm. The chemical composition of substrate is presented in Table 1 and is in accordance with manufacturer's certificate.

Zirconium carbide (ZrC) powder characterised by density of 6.73 g/cm^3 was used to produce pre-coat. The morphology of ZrC powder particles was observed in scanning electron microscopy (SEM) and is presented in Fig. 1a. ZrC particles were characterised by irregular shape, and the average particle size (APS) was less than 15 µm. The ZrC powder purity was 99.9%.

2.2 Fe/ZrC production parameters

Prior to the study, the substrate material was ground, next cleaned using alcohol, and finally etched with acetone. In the first step of coating production, ZrC pre-coat in the form of paste was produced. This paste consisted of ZrC powder as base material and solution of sodium water glass with distilled water as a binder. The consistency of the paste is crucial in the context of its application on steel substrate. Too liquid a paste does not allow for the formation of a thick pre-coat. However, when the paste is too dry, it is difficult to distribute it evenly and significant differences in thickness are observed over the entire surface of the sample. In this study paste was prepared using 62.50 wt. % ZrC powder, 18.75 wt. % water glass, and 18.75 wt. % distilled water. The same paste composition was used in the preliminary tests involving the analysis of single-laser tracks, which was described by Bartkowski in the paper [17]. The prepared paste was applied to the steel substrate with a brush. In order to obtain a thick pre-coat, the application process had to be repeated several times. A single application of paste by brush made it possible to obtain about 50 µm thickness. The thicknesses of all pre-coats were measured after each subsequent layer dried. To pre-coat thicknesses measure a Posi-Tector® 6000 Advance ultrasonic sensor with an accuracy of ± 2 µm was used. In order to accurately check pre-coat thicknesses, cross-sections were also observed selectively in SEM (Fig. 1b–d). Only those pre-coats with a similar thickness over the entire surface of the specimen were submitted for laser processing.

Fe/ZrC coatings were produced by laser remelting of three types of ZrC pre-coat with thicknesses of 100 µm, 150 µm, and 200 µm. Laser processing was performed using TruDiode 3006 diode laser with a nominal power of 3 kW. The laser head movement was controlled by a 5-axis KR16-2 robotic arm from KUKA. Three laser beam powers (500 W, 700 W, 900 W) were used to determine the impact of the

Table 1 Chemical composition of 145Cr6 steel used in study [wt%]

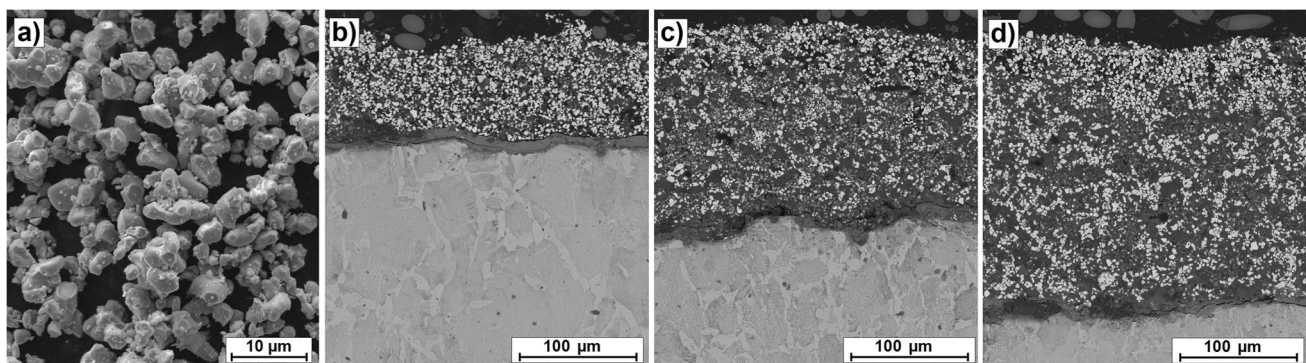| C	Mn	Si	P	S	Cr	V	Fe
1.35	0.60	0.30	0.02	0.02	1.45	0.20	bal

Fig. 1 Morphology of powder and pre-coats: **a** ZrC powder particles, **b** ZrC pre-coat 100 µm, **c** ZrC pre-coat 150 µm, ZrC pre-coat 200 µm

laser beam power on the behaviour of the pre-coat and the steel substrate. Laser beam scanning speed was constant in all processes and was 3 m/min. The laser beam diameter was 1 mm. The laser beam wavelength was 1040 nm, while electromagnetic mode of this laser was TEM_{00}. The distance between the laser head tip and the surface of applied pre-coat was constant and was 60 mm. Laser processing parameters and specimen designation are shown in Table 2.

The process of coating production consisted in moving a laser beam from one edge of the specimen to the other, and turning off the laser. Then laser head returned to the start point, next it was transferred transversely by 0.5 mm. The laser was turned on and the first move was repeated. This movement of laser head was repeated until the remelting of the entire specimen surface. The laser track overlap was

50%. The procedure was the same as in the study described by Bartkowski et al. in paper [23], where the authors focused on production of ZrC coatings on Monel-400 alloy. A description of laser processing is presented in the schematic in Fig. 2.

2.3 Microstructure investigation

Microstructure examination was carried out on cross-section of produced coatings. Two models of Schottky field emission gun scanning electron microscopes (FEG SEM): MIRA3 from TESCAN and JSM-7600F from JEOL were used. Depending on the microscope, 10 kV and 15 kV acceleration voltage, respectively, was used. Specimens of Fe/ZrC composite coatings were ground and polished using a Mecatech 250 device from PRESI. Grinding and polishing discs dedicated to hard materials were used. In order to reveal the microstructure of produced coatings, the cross sections were etched in 5% HNO_3 solution for 45 s.

2.4 Chemical and phase composition study

In order to determine the chemical compositions of Fe/ZrC composite coatings, energy dispersive X-ray spectroscopy (EDS) was applied. The study results were presented in the form of mapping of chemical elements and EDS point analysis. These results were related to the phase composition obtained during X-ray diffraction (XRD) tests. PANalytical EMPYREAN X-ray diffractometer with an automated sample feeding table was used to identify the phases. The study

Table 2 Parameter of laser processing

Specimen number	Pre-coat thickness [μm]	Laser beam power [W]	Laser beam power density [W/mm²]
1A	100	500	636.9
1B	100	700	891.7
1C	100	900	1 146.5
2A	150	500	636.9
2B	150	700	891.7
2C	150	900	1 146.5
3A	200	500	636.9
3B	200	700	891.7
3C	200	900	1 146.5

Fig. 2 Scheme of Fe/ZrC coating production: **a** preparation of the ZrC pre-coat and thickness control and **b** laser processing—cross section across the laser tracks
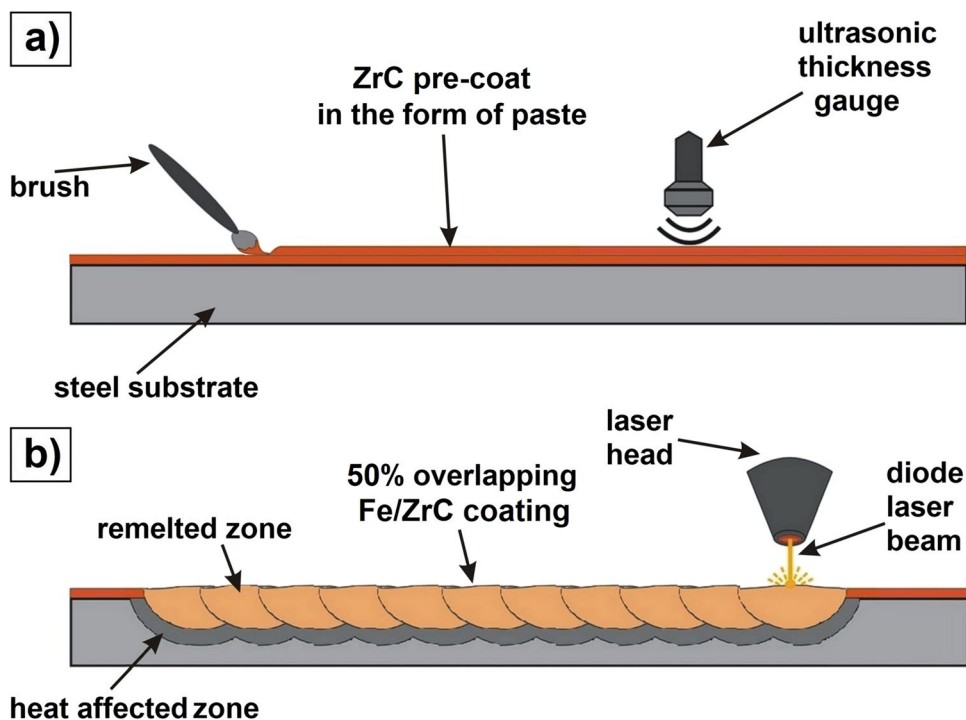
was carried out using an X-ray ceramic lamp with Cu anode. A voltage of 45 kV and a current of 40 mA were applied, and the temperature during tests was 25 °C.

2.5 Microhardness tests

Microhardness tests of Fe/ZrC coatings were carried out on cross sections perpendicular to coating from the surface to the core unmodified by laser beam using FM-810 microhardness tester from Future-Tech equipped with FT-Zero automatic indentation measuring software. The Vickers method was applied. Each indentation was made using a load of 50 g and loading time of 15 s. The results of the obtained tests allowed for creation of microhardness profiles. The aim of microhardness tests was to check whether a smooth transition between the substrate and the coating would be obtained. The hardness of ZrC is known (above 2500 HV), so it was necessary to check whether the laser beam will allow mitigating the sudden change of hardness in relation to the steel substrate. To ensure that the microhardness is uniform in individual zones distant from the surface, measurements were made both in the axis of the laser tracks and in the area of overlapping area.

2.6 Corrosion resistance tests

For tests of corrosion resistance 3.5% NaCl aqueous solution was applied. Potentiostat–galvanostat ATLAS 1131 EU&IA from Atlas-Sollich was used. The tests were conducted in accordance with the PN-EN ISO 17475 standard. The same surface roughness is necessary for the correct performance of corrosion tests; therefore, the specimens were ground to obtain Ra = 1.24 μm. The potentiodynamic method using anodic polarisation curves was applied. These tests were performed keeping the constant temperature of solution (22 °C) and using a sweep rate of 0.5 mV/s. Saturated calomel electrode (SCE) as reference electrode and platinum as auxiliary electrode were applied. The aim of the study was to determine the influence of laser beam power and the pre-coat thickness on corrosion resistance of the Fe/ZrC coating produced. The corrosion potential and corrosion current values obtained by Tafel extrapolation were used to evaluate these properties. The shape of the obtained polarisation curves was also analyzed.

2.7 Wear resistance tests

Amsler-type method was applied to carry out wear resistance tests. Tribotester MBT-01 was used. The specimen for testing was a plate with a produced Fe/ZrC composite coating, while a counter specimen was a ring made of Hardox®450 with a hardness of 35 HRC. Dry friction conditions and the following parameters were used: rotation speed of counter-specimen: 250 rpm, force pressure on the specimen: 147 N. The friction period lasted 60 min, and the mass loss of specimen was checked every 10 min, taking the measurements with the AS220.R2 analytical balance from RADWAG. In addition, observations of the surface after wear tests using SEM were performed. The purpose of wear resistance tests was to find a correlation between laser beam power, thickness of pre-coat, microhardness, and friction effects on the produced Fe/ZrC composite coatings.

3 Results of studies

3.1 Microstructure analysis

Immediately after the production of the Fe/ZrC composite coatings, they were observed both with the naked eye and with a stereoscopic microscope. The produced coatings were characterised by a very similar width of laser tracks. No significant differences in colour were observed. No porosity was observed on the surface of any of the coatings, but cracks were found on the coatings produced with the pre-coat of the highest thickness. The largest number of cracks occurred in Fe/ZrC coatings produced with a laser beam power of 500 W. The cracks ran along the axis of the tracks (faces of the produced tracks). Increasing laser beam power significantly reduced the number of cracks. A maximum laser beam power of 900 W contributed to almost complete reduction of this phenomenon. Increasing the power of laser beam caused an increase in temperature of the process. It also increased the share of the substrate in the produced coating. Increasing the amount of base material led to a decrease in the brittleness of the coating. Macroscopic observations of the remaining composite coatings, regardless of laser beam power applied and pre-coat thickness produced, did not show any defects on the surface.

In order to accurately assess the impact of the applied manufacturing method and its initial parameters on the final Fe/ZrC composite coatings, microscopic examinations were carried out using scanning electron microscopy. The morphology of Fe/ZrC composite coatings produced with all analysed parameters is shown in Fig. 3. It can be stated that the thickness of the coatings depends both on laser beam power used and pre-coat thickness. The application of a 100 μm pre-coat thickness resulted in the smallest thickness of the final Fe/ZrC composite coating. The thickness values given below result from the arithmetic mean calculated from 10 measurements, 5 in the track axis and 5 in the area of their overlap. Both the thickness of the coating from the surface to the visible parabolic remelting line as well as the thickness of the heat-affected zone were measured. Depending on the power of the laser beam, they were, respectively, 221 μm and 254 μm (for 500 W, Fig. 3a) and 256 μm and 252 μm (for
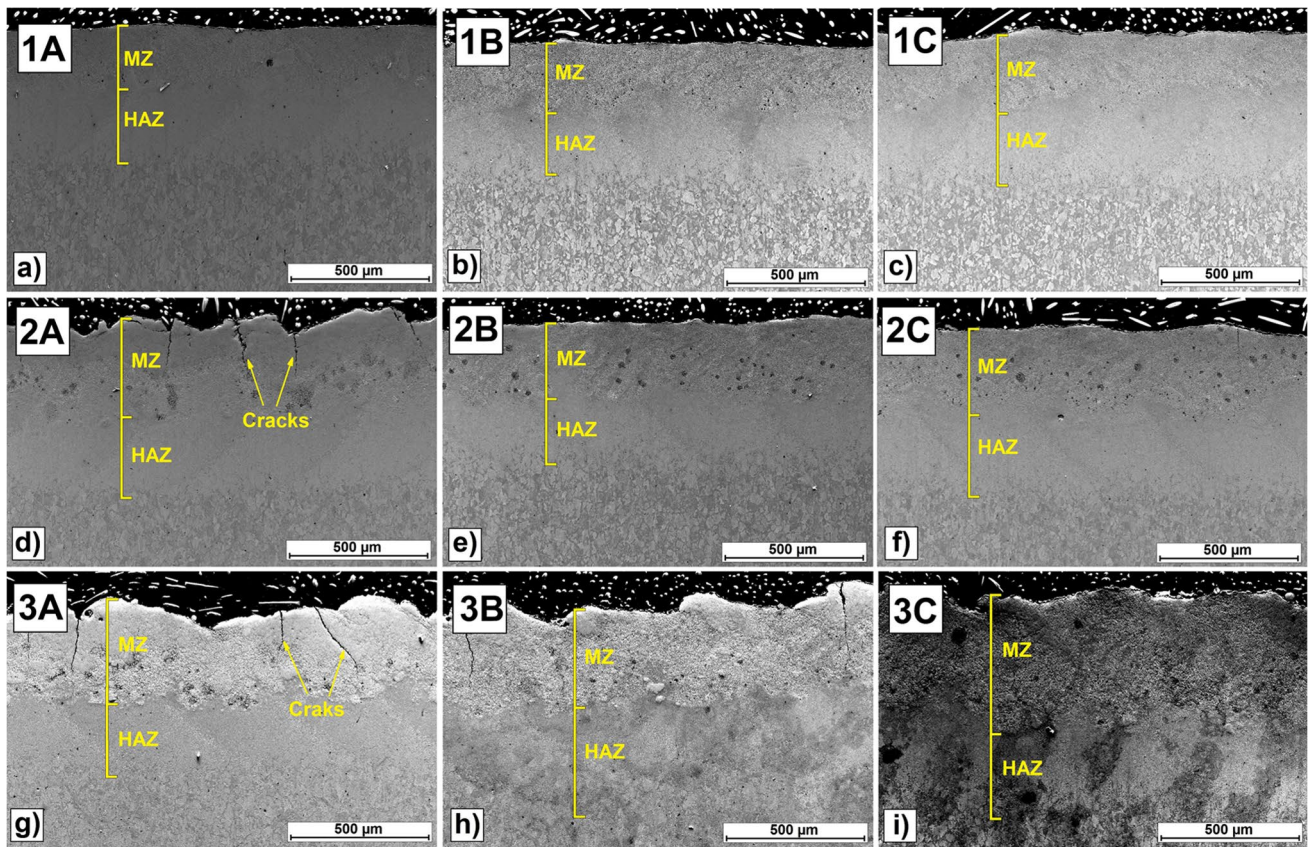
Fig. 3 Microstructure of Fe/ZrC coatings produced using different parameters of pre-coat thickness and laser beam power—designations from 1A to 3C according to Table 2. MZ, melted zone; HAZ. heat-affected zone

700 W, Fig. 3b). As can be seen, the increase in laser beam power from 500 to 700 W caused only slight changes in the thickness of the HAZ. On the other hand, visible changes in the thickness of individual zones resulted from the use of the highest laser beam power, respectively, 275 μm and 279 μm (for 900 W, Fig. 3c). It was demonstrated that Fe/ZrC coatings produced by remelting a pre-coat of 100 μm thickness are well bonded to the steel substrate. Due to the use of steel with a high carbon content as the substrate, three zones can be identified on the cross-section of the specimens (viewed from the right side in Fig. 4): the substrate with a perlitic structure, the heat-affected zone with a martensitic structure, and the composite coating. The sub-substrate zone of the composite coating is characterised by the presence of a martensitic matrix, which disappears with increasing the amount of the ZrC reinforcing phase. Produced coatings do not show porosity, cracks, or delaminations or discontinuities of the material at the coating/substrate boundary.

As for ZrC composite coatings obtained by laser beam remelting of pre-coat of 150 μm thickness, similar relationships between the thicknesses of individual zones can be observed. For coatings produced with a laser beam power of 500 W and 700 W, the average thickness of the remelted

zone was 300 μm, and the heat-affected zones were 248 μm and 242 μm, respectively. Only an increase in laser beam power to 900 W increased the remelting zone to 344 μm and the heat affected zone to 270 μm. However, distinct differences in the structure of the produced coatings were observed. The use of the lowest laser beam power caused problems with producing a coating with an even surface. Cracks were observed in it from the surface towards the base. This was due to too many carbide particles compared to the amount of iron in the substrate. This resulted in the lack of an adequate amount of matrix which would constitute a binding phase for hard particles. It should also be taken into account that the pre-coat material was subjected to cyclic heating and cooling as a result of the laser beam action. This heating, however, was not sufficient enough to melt the carbides, but it was enough to subject them to thermal shock and cause them to crack. The successive cyclic heating and cooling contributed to the formation of cracking focuses, and these cracks propagated further into the composite coating during the cooling process. Increasing laser beam power to 700 W and further to 900 W contributed to a reduction in all microstructural defects. The surfaces became even, no cracks and porosity were observed, and an
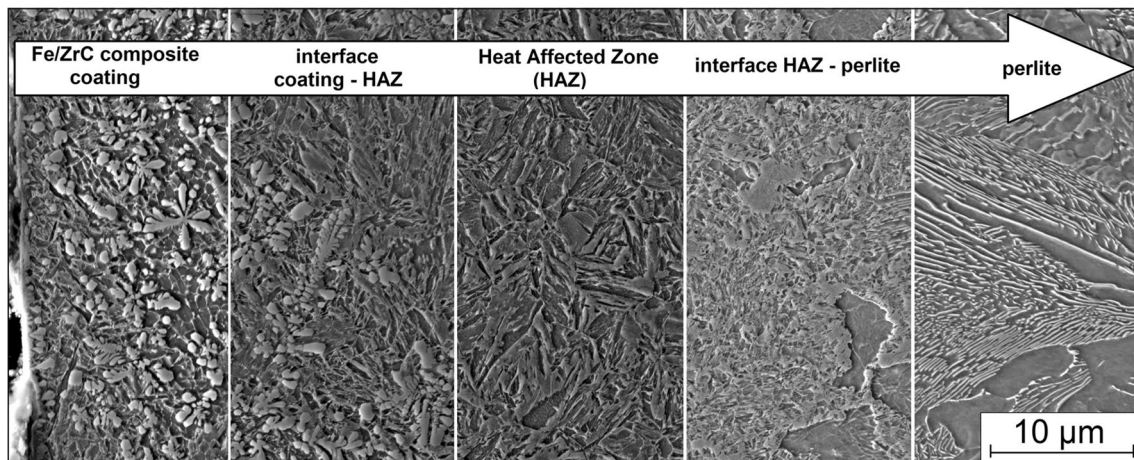
Fig. 4 Coating-substrate interface of Fe/ZrC composite coating produced using 500 W and 100 µm of ZrC pre-coat

additional effect was very good bonding of the coating with the steel substrate.

When a 200 µm pre-coat thickness was used, the only laser beam power parameter that allowed the coating to be produced without microstructural defects was 900 W. The lower the laser beam power, the more defects were observed in the form of cracks and unevenness on the coating surface. The use of the thickest pre-coat resulted in the thickest final Fe/ZrC composite coatings. In the coatings produced at the power of 500 W and 700 W, the average thickness of the remelted zone was 345 µm and 373 µm, respectively, and the heat affected zones did not differ significantly amounting to 268 µm and 264 µm, respectively. Increasing laser beam power to 900 W caused a significant increase in the average thickness of the remelted zone to 482 µm and in the heat-affected zone to 326 µm. By analysing all the produced coatings, it can be concluded that the phenomenon of agglomeration of ZrC particles was not observed, which favoured a uniform distribution of the reinforcing phase. ZrC density does not differ significantly from the density of iron, which also had a positive effect on coating structures. Too high or too low a density of the reinforcing phase may result in particles falling into the molten metal pool throughout the process or particles flowing to the pool surface.

Additional microscopic examinations were carried out at high magnification. The results of the microstructure tests are presented in Figs. 5, 6, and 7. The middle areas of the remelted zone were selected. In Fig. 5a Fe/ZrC composite coating is shown, which was produced by remelting a 100-µm-thick pre-coat with three 500 W laser beam powers (Fig. 5a, d), 700 W (Fig. 5b, e), and 900 W (Fig. 5c, f). Dendritic carbide precipitations that nucleate on primary ZrC particles were found. The mechanism of formation of such a structure was described in the previous paper of the authors [13] and consists in a complete remelting of the smallest

carbide particles, and in nearly complete remelting of larger carbide particles. Laser beam acts on the substrate, melts it, and causes mixing of remelted and partially remelted carbides with the substrate. Steel substrate is enriched with zirconium and carbon. In results of this new carbide phases were formed. In Fig. 5d it can be very well seen that the nucleation site of dendritic secondary carbides is unmelted primary carbide ZrC. However, Fig. 5e shows unmelted primary carbides of less than 2 µm, which act as crystallisation nuclei. The eutectic is also visible. All attached microstructures in Fig. 5 show a very tight packing of carbide phases in the remelted zone of the coating. No discontinuities of material, porosity, or cracking are observed.

Increasing pre-coat thickness to 150 µm had a distinct effect on the microstructure obtained (Fig. 6a–f). A higher number of ZrC particles absorb laser beam heat more intensely; therefore, the use of the same powers no longer allows for complete remelting of most ZrC particles. When using a 500 W laser beam power, non-full remelted ZrC particles up to about 6 µm in size are visible (Fig. 6a). Increasing the power resulted in greater remelting of ZrC particles, as visible in Fig. 6b (700 W) and Fig. 6c (900W). High-magnification observations show that among the primary ZrC particles, there is an additional mesh that is a form of matrix of a eutectic structure (Fig. 6e). The highest laser beam power melted the ZrC particles quite substantially, which caused them to partially bond with each other (Fig. 6f).

The use of the greatest pre-coat thickness of 200 µm reduced the melting of the reinforcing phase even more. Figure 7a–f shows composite Fe/ZrC coatings produced at three laser beam powers by remelting a thick pre-coat in paste form. ZrC particles with very few partially melted edges and large sizes are visible (Fig. 7a). A fairly limited amount of the matrix is visible, which would include
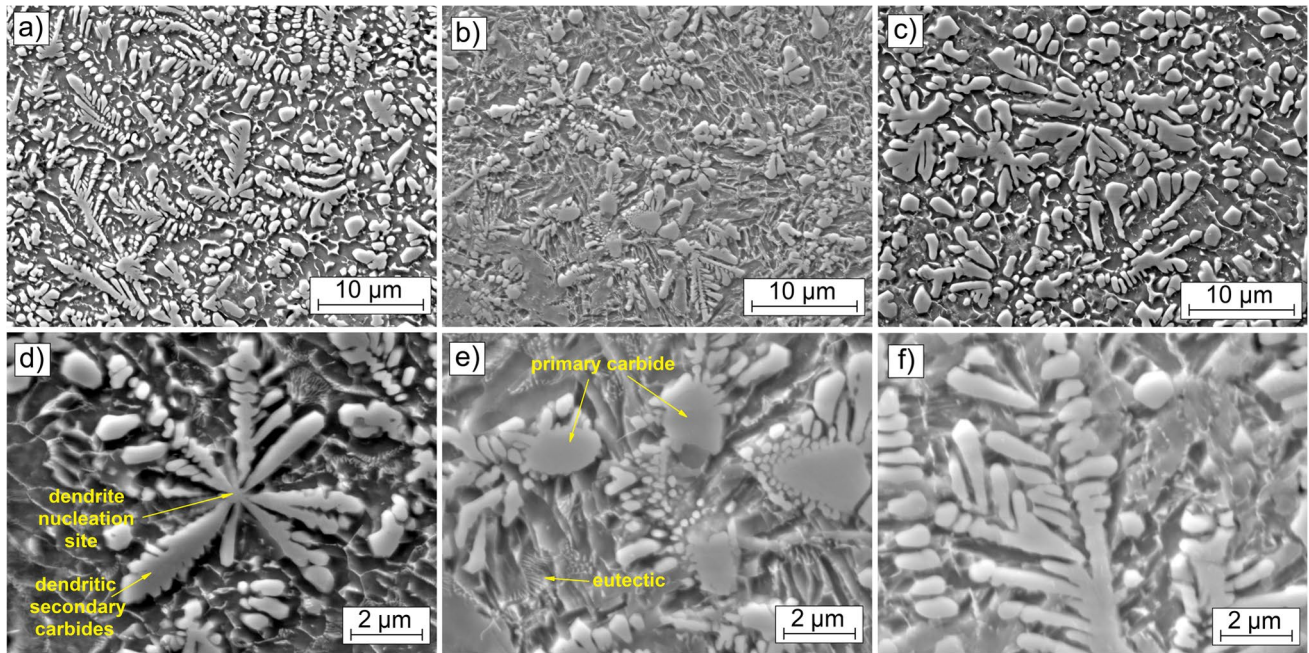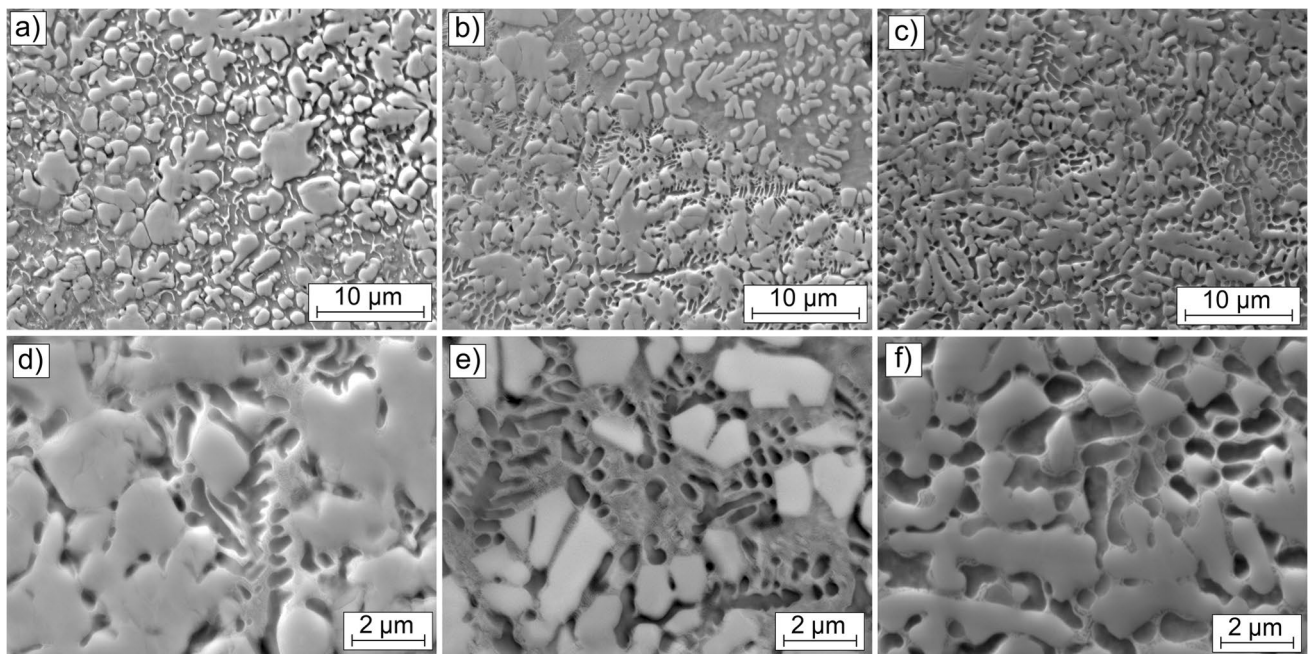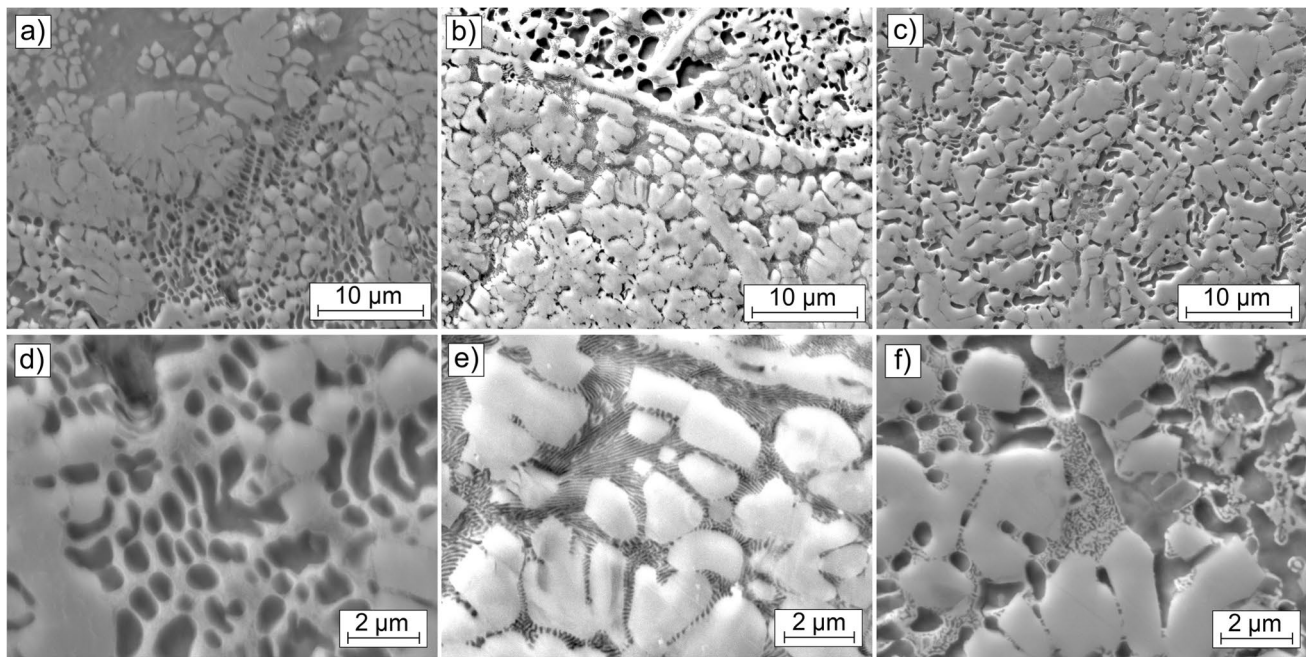
Fig. 5 Microstructure of the middle area of remelted zone for Fe/ZrC coating produced by remelted of 100 μm ZrC pre-coat and three laser beam powers: **a**, **d** 500 W; **b**, **e** 700 W; **c**, **f** 900 W

Fig. 6 Microstructure of the middle area of remelted zone for Fe/ZrC coating produced by remelted of 150 μm ZrC pre-coat and three laser beam powers: **a**, **d** 500 W; **b**, **e** 700 W; **c**, **f** 900 W

elements derived from the substrate material (mainly iron). Increasing laser beam power increases partial melting of ZrC particles and their bonding. Comparing the coatings produced at different thicknesses of the pre-coat, it can be concluded that increasing their thicknesses leads to an increase in the amount of the reinforcing phase. At the greatest thickness, a significant dominance of ZrC particles in relation to the matrix is observed (Fig. 7c). Observation of the microstructure obtained with the greatest thickness of the pre-coat can lead to an impression that

Fig. 7 Microstructure of the middle area of remelted zone for Fe/ZrC coating produced by remelted of 200 μm ZrC pre-coat and three laser beam powers: **a**, **d** 500 W; **b**, **e** 700 W; **c**, **f** 900 W

a coating resembling sintered carbide was formed on the steel surface.

For all coatings produced, a lamellar eutectic structure in the matrix was identified when observed in large magnification (Fig. 8). Their formation is associated with rapid heating and cooling, which accompanies laser processing. For example, three types of Fe/ZrC composite coatings produced with the same 700 W laser beam power but with different ZrC pre-coat thicknesses were compared. Lamellar structure plates were of nanometric sizes. In a 100-μm pre-coat the average width of the lamella is about 80 nm (Fig. 8a).

As the thickness of the coating increased and thus the amount of ZrC, lamella width decreased, reaching values of approximately 60 nm for the pre-coat of 150 μm and 40 nm for the pre-coat of 200 μm. Reducing eutectic dimensions resulted from greater super cooling of the material. Laser beam power, and thus the heat delivered, was the same; however, the speed of its dissipation was higher where there was a greater share of the high-melting reinforcing phase.

3.2 Chemical and phase composition results

The XRD spectra for the produced Fe/ZrC composite coatings with different laser beam parameters and different pre-coat thicknesses are shown in Fig. 9.

Three phases were identified on the coatings: zirconium carbide (ZrC), iron (Fe), and Fr_2Zr, which are Laves phases. The occurrence of such phases while iron, zirconium, and carbon are bonded is confirmed by researchers in the article

[25], where thermodynamic calculations of the Fe–Zr–C system are presented. It should be noted that no additional phases were identified in the tests, which may indicate that secondary carbides formed are also zirconium carbides. It was found that the thickness of the ZrC pre-coat had a significant impact on phase intensity. At the lowest pre-coat thickness, regardless of laser beam power, the Laves Fe_2Zr phase was not identified. The intensity of the ZrC reinforcing phase was also lower. There was a clear dominance in the intensity of alpha iron phase derived from the substrate. As coating thickness increased, and thus the amount of ZrC, the Laves phase Fe_2Zr began to appear, its intensity was low. However, the intensity of the ZrC phase increased quite significantly, which the authors expected already in microstructure observation. The highest intensity of the ZrC phase was achieved at the thickest pre-coat. There was no significant influence of laser beam power on the intensity of individual phases. Laser beam power was selected in such a way as to preserve the composite character of the coatings produced. Based on the Fe–Zr–C equilibrium graphs, it is assumed that the use of much higher laser beam powers, which would result in intensive mixing of the pre-coat with a large amount of steel substrate, would contribute to the identification of a variety of other phases. However, this might result in a departure from the composite coating structure, in which the reinforcing phase can be clearly separated from the matrix.

Chemical composition tests were performed using the EDS method. Three basic chemical elements included in the produced coatings, i.e. iron, zirconium, and carbon, were
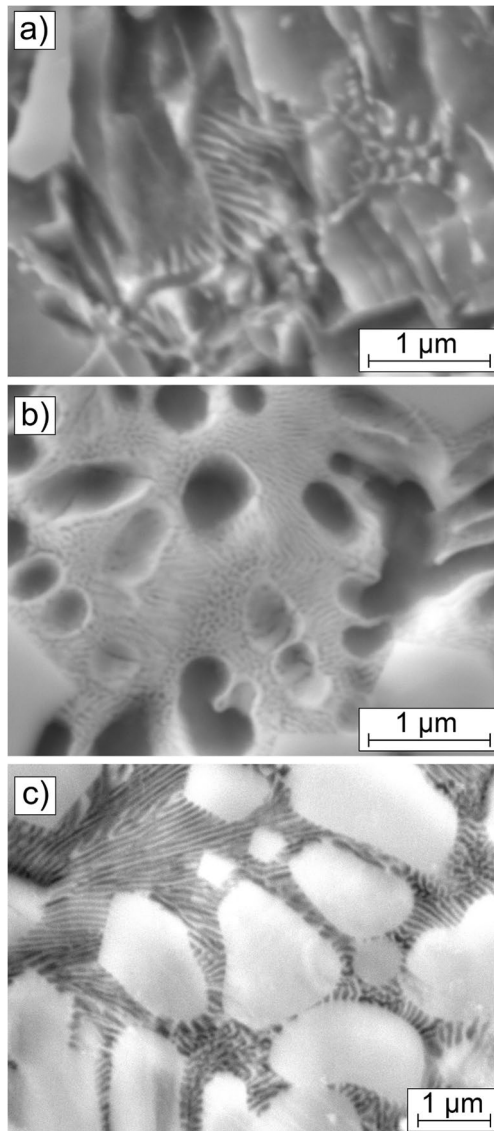
Fig. 8 Microstructure of Fe/ZrC coating produced with a laser beam power of 700 W and different thicknesses of ZrC pre-coat: **a** 100 μm, **b** 150 μm, **c** 200 μm

analyzed. In Fig. 10 the measurement sites, while in Table 3 the results of chemical composition tests for the Fe/ZrC coating produced by remelting the 150-μm pre-coat with three different laser beam powers are presented.

It was found that the matrix formed in laser beam remelting is made of iron and zirconium, but the increase in laser beam power causes an increase in the share of iron in this matrix. This is due to greater remelting of the steel substrate. In the matrix (dark areas) of the coating produced at 500 W (Fig. 10a), the ratio of iron to zirconium is about 3:2 in the majority of the sites studied. On the other hand, the increase in power to 700 W and further to 900 W caused that these proportions changed significantly. In some areas the

proportion of iron was observed at the level exceeding 90%. It should be mentioned that all tested sites were located in the central part of the Fe/ZrC composite coatings produced. This indicates a very good mixing of the pre-coat with the steel substrate, which was influenced by strong convection movements called Marangoni flows. Analysis of the chemical composition at points of bright areas on micrographs confirms the occurrence of phases containing large amounts of zirconium and carbon. It is a reinforcing phase introduced in the primary form and precipitating secondary from liquid alloy in the form of zirconium carbide.

Exemplary areas from the remelted zone for each of the produced Fe/ZrC coatings are shown in Fig. 11 as EDS mapping. The distribution of individual elements was applied to SEM images. Studies confirm a high zirconium share in the reinforcing phase and dendritic precipitates, and iron-enriched matrix of a cellular structure or in a mesh form.

3.3 Microhardness observations

In Fe/ZrC coatings, due to a relatively high proportion of the reinforcing phase and numerous precipitates of secondary carbides, there is no significant difference in microhardness measured in laser track axes and in the area of their overlapping. This proves a homogeneous hardness in individual depths of the coatings produced. Microhardness of individual composite coatings produced at different parameters is shown in Fig. 12.

The effect of laser beam power on the hardness obtained by remelting individual pre-coat thicknesses was tested. As for the lowest thickness, i.e. 100 μm, the highest hardness (approximately 840 HV0.05) was achieved with the highest laser beam power of 900 W. It should be noted here that the hardness was measured as far as possible ignoring primary ZrC particles. The hardness of the primary ZrC particles is known (2500 HV), so it was important to determine how the hardness of the matrix changed. A higher laser beam power caused remelting of fine carbide particles and enrichment of the matrix with carbon and zirconium. This was of great importance since the matrix, which was not enriched with these elements, was mainly built of iron derived from the substrate. Iron does not reach high hardness values; therefore, the maximum hardness values recorded for laser beam power of 500 W is approximately 680 HV0.05. When a laser beam power was 700 W, hardness of approximately 800 HV0.05 was achieved. This was slightly less than when a laser beam power was 900 W. Therefore, high hardness values can be obtained using a power 200 W less than the maximum, which can be considered in terms of energy savings.

It can be stated that the most favourable hardness values were obtained for the coatings produced by pre-coat remelting with a thickness of 150 μm. The value of 2200 HV0.05 was achieved here for laser beam power of 500 W. However,
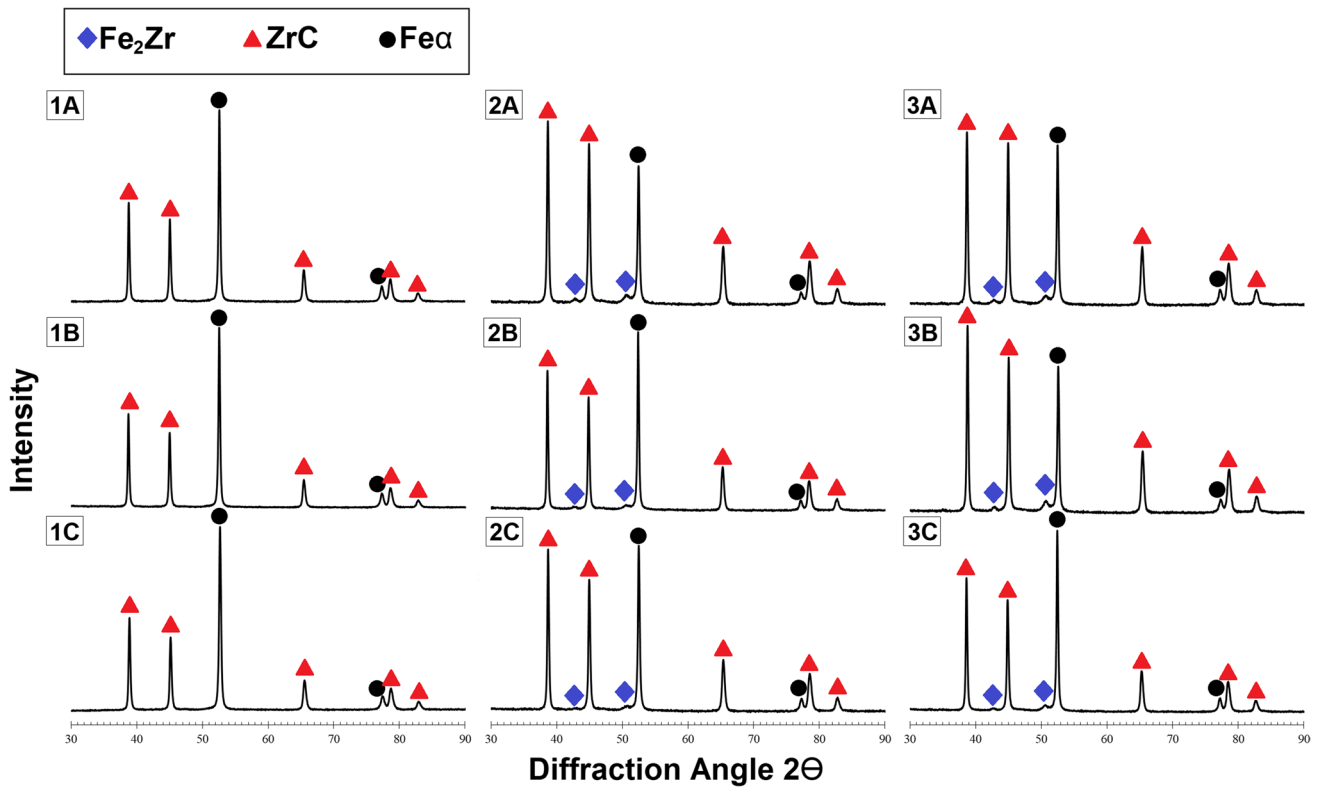
Fig. 9 XRD spectra Fe/ZrC coatings produced using different laser beam powers and different thicknesses of ZrC pre-coat—designations according to Table 2
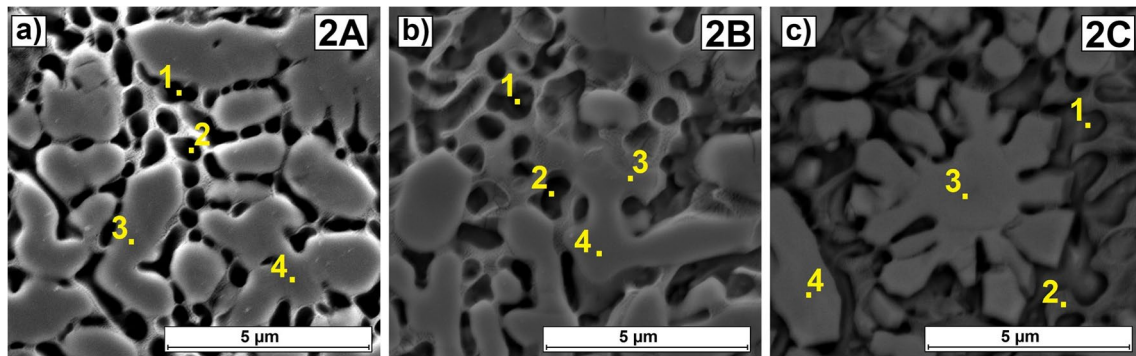

Fig. 10 Points of chemical composition analysis (EDS) for Fe/ZrC coatings produced by remelting of ZrC pre-coat of 150 μm and laser beam power of **a** 500 W, **b** 700 W, **c** 900

Table 3 Chemical composition of Fe/ZrC coating produced by remelting of ZrC pre-coat 150 μm with three different laser beam powers	Specimen number	2A				2B				2C			
	Analysis area	1	2	3	4	1	2	3	4	1	2	3	4
	Fe [wt.%]	46.8	54.0	77.8	74.8	89.6	89.6	49.9	77.0	94.4	56.6	79.8	71.7
	Zr [wt.%]	38.5	33.3	20.2	22.9	8.3	5.8	32.6	20.8	3.7	27.8	18.5	26.1
	C [wt.%]	14.7	12.7	2.0	2.3	2.1	4.6	17.5	2.2	1.9	15.6	1.7	2.2

Fig. 11 EDS mapping for the Fe/ZrC composite coating at different thicknesses of the initial coating and using different laser beam powers: **a** 100 μm and 500 W; **b** 100 μm and 700 W; **c** 100 μm and 900 W; **d** 150 μm and 500 W; **e** 150 μm and 700 W; **f** 150 μm and 900 W; **g** 200 μm and 500 W; **h** 200 μm and 700 W; **i** 200 μm 900 W
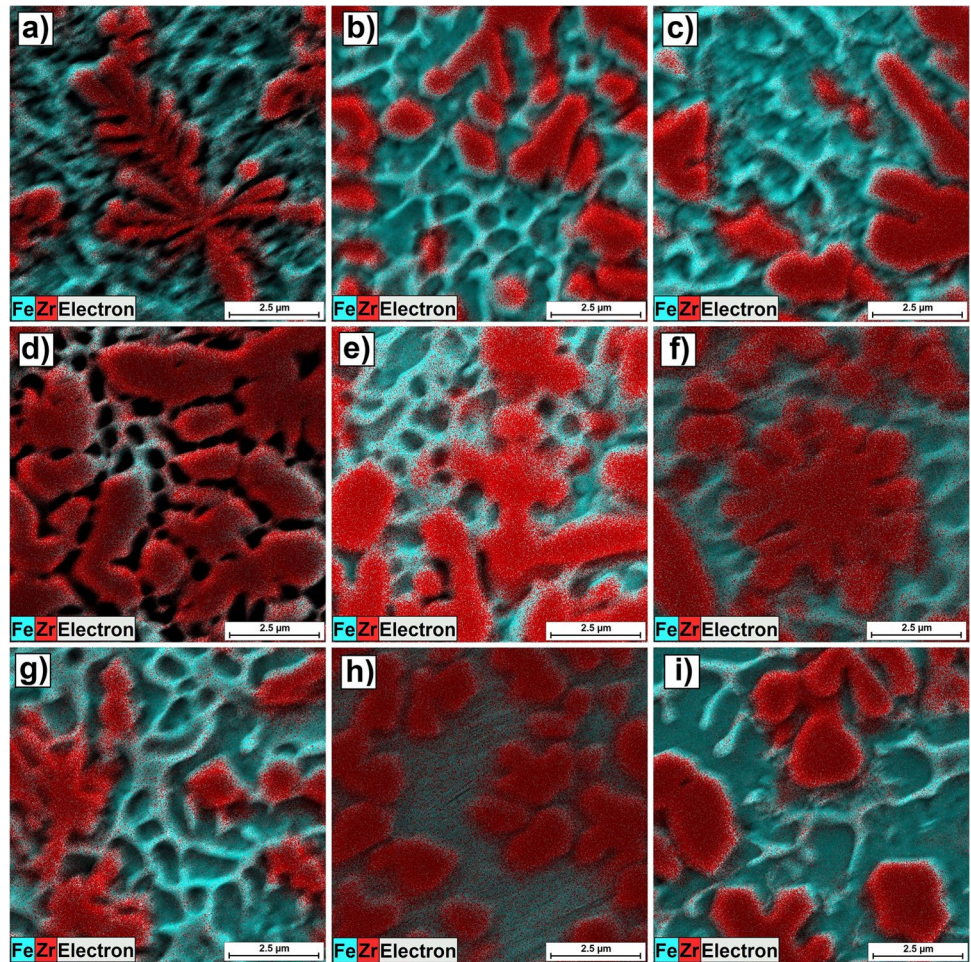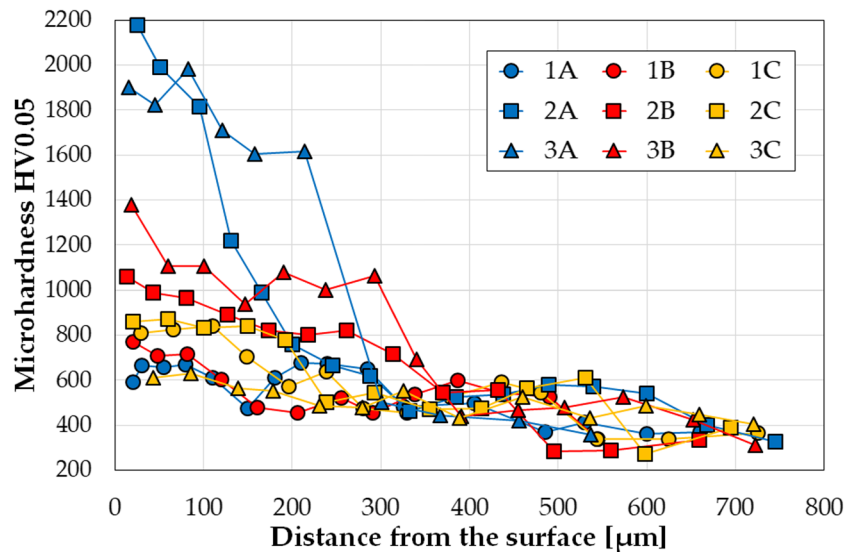

Fig. 12 Microhardness of Fe/ZrC coatings produced using different pre-coat thicknesses and different powers of the laser beam—designations according to Table 2

this hardness should be related to the microstructure and the cracks present in it, which disqualifies this coating in terms of operation. Increasing laser beam power to 700 W allowed obtaining a high hardness at the level exceeding

1000 HV0.05. Further increasing laser beam power to 900 W resulted in a hardness of approximately 800 HV0.05, i.e. hardness similar when the parameters were 100 μm and 700 W, respectively. Very promising hardness measurement

results were recorded for Fe/ZrC coatings produced by remelting a 200 μm pre-coat. The values obtained were at the level of 2000 HV0.05 (for 500 W) and 1400 HV0.05 (for 700 W). Analysing microhardness imprint distribution, it was found that the obtained hardness is the result of measurements made mainly in the presence of secondary carbide precipitates, around which a small amount of iron matrix was present. Also, attention should be paid to a very large number of cracks in the coatings produced with both parameters. Increasing laser beam power to 900 W made it possible to perform microhardness measurements within the matrix although this matrix was not quite enriched with carbides, hence the hardness of approximately 600 HV0.05.

Fig. 13 Corrosion resistance curves for Fe/ZrC coatings: **a** range − 1.5 to + 1.5 V, **b** enlarged area − 1.05 to − 0.80 V; designations according to Table 2

The lack of matrix enrichment in Zr and C might probably have been due to a large amount of ZrC, which took over laser beam heat. Laser treatment partially melted the steel substrate, but most of the heat was absorbed by the ZrC particles, and in the matrix iron predominance was observed, which was confirmed by the EDS mapping results.

3.4 Corrosion resistance

The results of electrochemical corrosion resistance tests of the Fe/ZrC coatings in a 3.5% NaCl solution are presented in the form of corrosion curves in Fig. 13.

No significant differences between the corrosion resistance of individual coatings was observed. Numerical values of current and corrosion potential are shown in Table 4. By enlarging corrosion curves (Fig. 13b) some differences in E_{corr} parameters can be observed. It is assumed that the graph leaning towards potential positive values characterises a material that is more corrosion resistant. Despite such minor differences, it can be concluded that the coatings produced with laser beam power of 700 W are most corrosion resistant. It should be noted that the pre-coat of 150 μm gave the best results. In light of the fact the pre-coat of 200 μm had cracks that had a negative impact on corrosion resistance, the second best composite coating Fe/ZrC was the one obtained with a pre-coat thickness of 100 μm. Corrosion resistance of the other coatings was lower. Therefore, it can be concluded that laser beam power, which contributes to structural changes responsible for corrosion phenomena, has a highly significant impact on corrosion resistance.

It was presumed that increasing laser beam power reduces corrosion resistance due to an increased remelting of the substrate and thus a higher amount of iron in the Fe/ZrC coating. This may be related to increasing potential difference in the coating being formed. The differences between individual elements are quite significant, as the potential of Zr is − 2.36 V, and Fe − 0.44 V. Thus, the Zr potential is more than five times lower than that of iron, and as it is widely known, the greater potential difference, the easier it is for electrochemical corrosion to occur. Increasing the amount of iron-containing matrix therefore leads to a decrease in corrosion resistance, which is also visible on micrographs made on the surface of coatings following corrosion tests. Figure 14 shows differences between
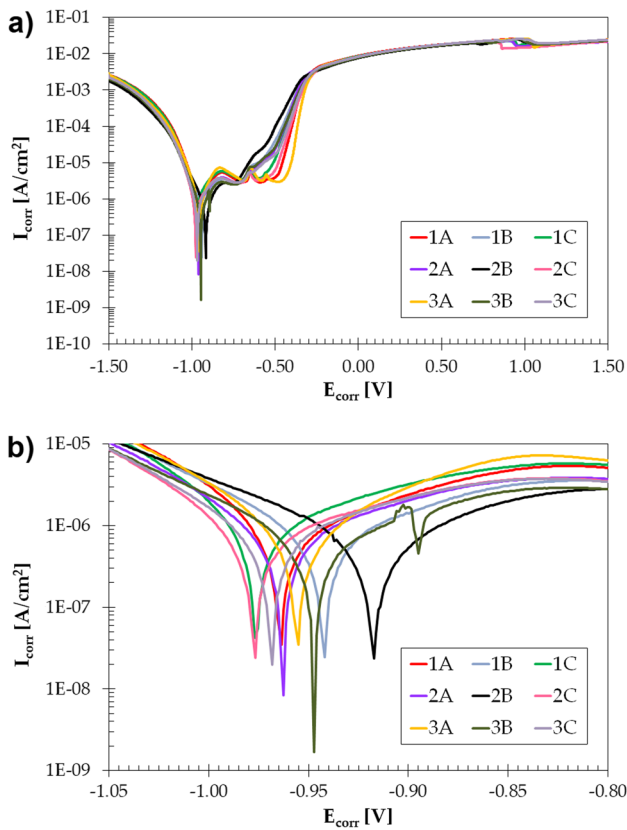
Table 4 Parameters obtained during corrosion tests of Fe/ZrC coatings produced using different laser beam powers and different thicknesses of pre-coat

Pre-coat thickness/laser beam power	500 W		700 W		900 W	
	E_{corr} (V)	I_{corr} (A/cm²)	E_{corr} (V)	I_{corr} (A/cm²)	E_{corr} (V)	I_{corr} (A/cm²)
100 μm	− 9.64 E − 01	7.11 E − 07	− 9.42 E − 01	6.38 E − 07	− 9.77 E − 01	1.04 E − 06
150 μm	− 9.62 E − 01	6.18 E − 07	− 9.17 E − 01	5.04 E − 07	− 9.77 E − 01	5.62 E − 07
200 μm	− 9.55 E − 01	8.91 E − 07	− 9.47 E − 01	5.67 E − 07	− 9.68 E − 01	6.83 E − 07

Fig. 14 Surface conditions after corrosion tests for Fe/ZrC coating produced by remelting of 150 μm pre-coat and laser beam power of **a** 700 W and **b** 900 W
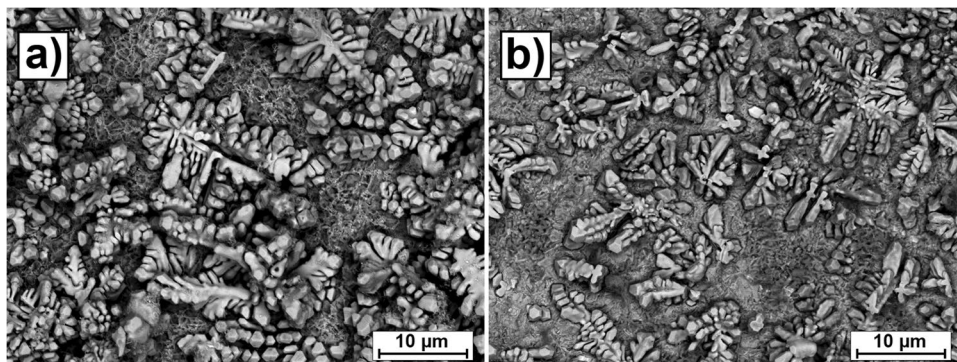
the surface condition after corrosion tests for the same pre-coat thickness (150 μm) and for laser beam power of 700 W (Fig. 14a) and 900 W (Fig. 14b).

A significant difference in the amount of the reinforcing phase in the form of primary and secondary ZrC particles is clearly visible. The surface with a larger amount of iron-containing matrix is subject to greater corrosion.

3.5 Wear resistance

Composite coatings are mainly produced in order to increase wear resistance. The introduction of hard reinforcing phases into the coating significantly extends product life cycle, which are most frequently tools working in the soil. The introduction of various types of carbides into the steel surface aims to carry out the same task. In Fig. 15, a wear resistance results of composite Fe/ZrC coatings produced at various laser beam powers and ZrC pre-coat thickness parameters in the form of dependence of mass loss as a function of time is shown. These graphs were related to wear

resistance of uncoated 145Cr6 steel in the state after hardening and low-temperature tempering.

It was found that formation of Fe/ZrC coatings significantly improves wear resistance compared to a steel substrate. The best of the produced composite coatings improved wear resistance more than threefold. In order to fully describe the graph, reference should be made to manufacturing parameters for each curve, as well as to the condition of the surface both prior to and following wear tests. Figure 16a–i shows a SEM image of the surface following dry friction tests. In terms of wear resistance the best coating produced is the Fe/ZrC coating formed as a result of remelting the 150-μm pre-coat with a 700 W laser beam. Here, the lowest sample weight loss was recorded, also its surface is not considerably damaged (Fig. 16e). Slightly worse surface condition appears to be that of the sample produced at the same pre-coat, but at a lower power of 500 W (Fig. 16d). However, it is most likely that due to relatively low remelting of ZrC particles, they tore out of the matrix and caused micro-cutting. The same mechanism was also described by other researchers during the production of coatings using laser technology [26, 27].

Fig. 15 Graph of mass loss versus friction time for Fe/ZrC coatings—designations according to Table 2
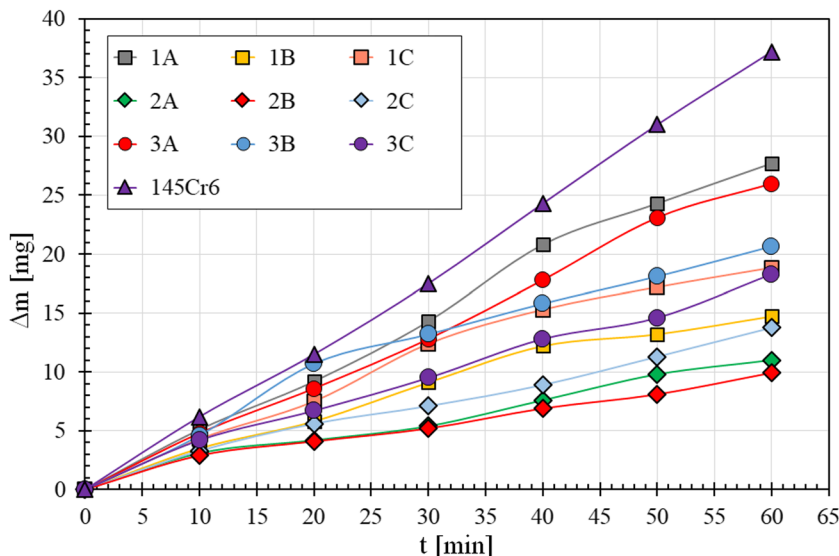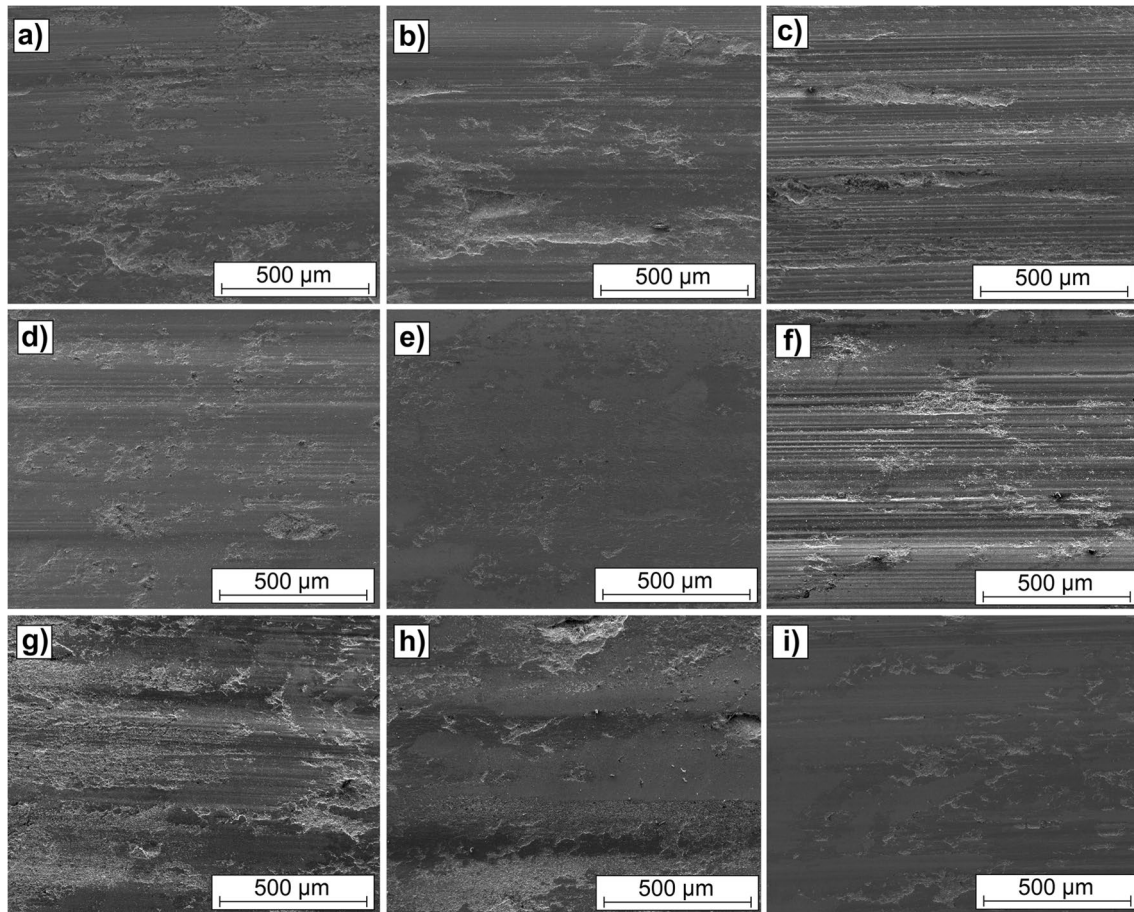
Fig. 16 Surface condition after wear tests for Fe/ZreC coatings produced using different parameters: **a** 100 μm and 500 W; **b** 100 μm and 700 W; **c** 100 μm and 900 W; **d** 150 μm and 500 W; **e** 150 μm and 700 W; **f** 150 μm and 900 W; **g** 200 μm and 500 W; **h** 200 μm and 700 W; **i** 200 μm 900 W

Micro-cutting was even better visible at laser beam power of 900 W (Fig. 16f). This sample, despite multiple wear traces, was characterised by one of the lowest weight losses (third in a row). Surface condition obtained immediately post-laser treatment also had quite a significant impact on wear resistance. Fe/ZrC composite coatings produced at the greatest pre-coat thickness (200 μm) might seem to be the most wear resistant. However, when laser beam powers of 500 W and 700 W were used, irregularities and cracks appeared on these coatings, which significantly deteriorated their wear resistance (Fig. 16g and h). Only an increase in power, a decrease in surface irregularities, as well as eliminating cracks allowed maintaining good wear resistance. Therefore, it should be emphasised that laser beam power is a very important parameter in laser processing of this type of coatings, which must be selected to match the pre-coat thickness. It cannot be too low, as it leads to problems with surface quality and problems of bonding the matrix with the reinforcing phase. It also cannot be too high, so as not to melt too much substrate, whose components have a lower hardness than the reinforcing phase.

4 Conclusions

Fe/ZrC composite coatings with a metallic matrix were produced on low-alloy steel by remelting the pre-coat in paste form, whose main component was ZrC powder. Three pre-coat thicknesses and three laser beam powers were used. The objective was to determine the influence of laser beam power on the behaviour of the "steel substrate–pre-coat" system and, as a result, to create a new, previously untested Fe/ZrC coating. It was found that it is possible to make a Fe-matrix coating, reinforced with ZrC on the steel surface of the sample by successive execution of laser tracks. In Bartkowski's earlier study, the author tested such possibilities on individual laser tracks. However, the execution of multiple tracks offered a wider look at the properties obtained. The main results can be summarised as follows:

1. As the pre-coat thickness increases, the thickness of the Fe/ZrC composite coatings also increases. Such a relationship was also observed when increasing laser beam power

for individual pre-coats. This is related to the supply of both a larger amount of additional material in the form of ZrC, as well as increasing the amount of heat supplied, i.e. operating on a larger amount of substrate material. However, both pre-coat thickness and laser beam power should be carefully selected in order to avoid any possible problems of coating cracking, which occurs when laser beam power is too low and pre-coats are too thick.

2. Laser treatment resulted in partial remelting of carbide particles characterised by larger size and complete melting of smaller ZrC particles, resulting in the precipitation of zirconium and carbon into the matrix. Enriching the matrix with these elements increased their hardness, among others.

3. It was found that the appropriate selection of laser beam power and pre-coat thickness can lead to an increase in wear and corrosion resistance. Incorrect parameter selection leads to drastic changes in friction wear resistance. The resistance deteriorates mainly due to the micro-cutting mechanism, which was promoted by the tearing hard carbide particles from the matrix.

Declarations

References

1. Kruusing A (2008) Handbook of liquids-assisted laser processing. Book, Elsevier, ISBN 978-0-08-044498-7. https://doi.org/10.1016/B978-0-08-044498-7.X5001-8

2. Steen WM, Mazumder J (2010) Laser material processing, 4th edn. Springer, London, UK. https://doi.org/10.1007/978-1-84996-062-5

3. Lawrence JR, Waugh D (2014) Laser surface engineering: processes and applications. In: Woodhead Publishing Series in Metals and Surface Engineering Book, 1st ed.; Kindle Edition, Elsevier, Amsterdam, The Netherlands

4. Schaaf P (2010) Laser processing of materials: fundamentals, applications and developments; Springer Series in Materials Science, vol. 139, Springer: Berlin/Heidelberg, Germany; GmbH & Co. KG: Berlin, Germany

5. Przestacki D, Kukliński M, Bartkowska A (2017) Influence of laser heat treatment on microstructure and properties of surface layer of Waspaloy aimed for laser-assisted machining. Int J Adv Manuf Technol 93:3111–3123. https://doi.org/10.1007/s00170-017-0775-2

6. Bartkowska A, Bartkowski D, Swadźba R, Przestacki D, Miklaszewski A (2018) Microstructure, chemical composition, wear, and corrosion resistance of FeB–Fe2B–Fe3B surface layers produced on Vanadis-6 steel using CO2 laser. Int J Adv Manuf Technol 95:1763–1776. https://doi.org/10.1007/s00170-017-1304-z

7. El-Labban HF, Mahmoud ERI, Al-Wadai H (2015) Formation of VC-composite surface layer on high C-Cr bearing tool steel by laser surface cladding. J Manuf Processes 20:190–197. https://doi.org/10.1016/j.jmapro.2015.08.004

8. Perrin T, Achache S, Meausoone PJ, Sanchette F (2021) Characterization of WC-doped NiCrBSi coatings deposited by laser cladding; effects of particle size and content of WC powder. Surf Coat Technol 425:127703. https://doi.org/10.1016/j.surfcoat.2021.127703

9. Huebner J, Rutkowski P, Kata D, Kusiński J (2017) Microstructural and mechanical study of Inconel 625 – tungsten carbide composite coatings obtained by powder laser cladding. Arch Metall Mater 62:531–538. https://doi.org/10.1515/amm-2017-0078

10. Bartkowski D, Młynarczak A, Piasecki A, Dudziak B, Gościański M, Bartkowska A (2015) Microstructure, microhardness and corrosion resistance of Stellite-6 coatings reinforced with WC particles using laser cladding. Opt Laser Technol 68:191–201. https://doi.org/10.1016/j.optlastec.2014.12.005

11. Bartkowski D, Kinal G (2016) Microstructure and wear resistance of Stellite-6/WC MMC coatings produced by laser cladding using Yb:YAG disk laser. Int J Refract Metals Hard Mater 58:157–164. https://doi.org/10.1016/j.ijrmhm.2016.04.017

12. Bartkowski D, Bartkowska A (2017) Wear resistance in the soil of Stellite-6/WC coatings produced using laser cladding method. Int J Refract Metals Hard Mater 64:20–26. https://doi.org/10.1016/j.ijrmhm.2016.12.013

13. Bartkowski D, Bartkowska A, Jurči P (2021) Laser cladding process of Fe/WC metal matrix composite coatings on low carbon steel using Yb: YAG disk laser. Opt Laser Technol 136:106784. https://doi.org/10.1016/j.optlastec.2020.106784

14. Schwanekamp T, Marginean G, Reuber M (2019) Laser beam melting of Cr3C2-NiCr. Int J Refract Metals Hard Mater 85:105069. https://doi.org/10.1016/j.ijrmhm.2019.105069

15. Bartkowska A (2021) Characteristics of Cr-B coatings produced on vanadis® 6 tool steel using laser processing. Materials 14:2621. https://doi.org/10.3390/ma14102621

16. Bartkowski D (2021) Manufacturing technology and properties of Fe/TaC metal matrix composite coatings produced on medium carbon steel using laser processing—preliminary study on the single laser tracks. Materials 14:5367. https://doi.org/10.3390/ma14185367

17. Bartkowkski D (2022) Influence of laser beam power on microstructure and microhardness of Fe/ZrC coatings produced on steel using laser processing—preliminary study on the single laser tracks. Materials 15:758. https://doi.org/10.3390/ma15030758

18. Lv X, Zhan Z, Cao H, Guo C (2020) Microstructure and properties of the laser cladded in-situ ZrB2-ZrC/Cu composite coatings on copper substrate. Surf Coat Technol 396:125937. https://doi.org/10.1016/j.surfcoat.2020.125937

19. Yong YW, Fu W, Deng QL, Yang JG (2017) Mechanism of Zr in in situ-synthesized particle reinforced composite coatings by laser cladding. Rare Met 36:934–941. https://doi.org/10.1007/s12598-017-0944-3

20. King D, Middendorf J, Cissel K, Key T, Carney C (2019) Selective laser melting for the preparation of an ultra-high temperature ceramic coating. Ceram Int 45:2466–2473. https://doi.org/10.1016/j.ceramint.2018.10.173

21. Craciun V, McCumiskey EJ, Hanna M, Taylor CR (2013) Very hard ZrC thin films grown by pulsed laser deposition. J Eur Ceram Soc 33:2223–2226. https://doi.org/10.1016/j.jeurceramsoc.2013.01.001

22. Liu T, Niu Y, Pan X, Shi M, Zheng X, Yu J, Ding C (2019) Laser ablation behaviors of vacuum plasma sprayed ZrC-based coatings. J Am Ceram Soc 102:4247–4258. https://doi.org/10.1111/jace.16278

23. Bartkowski D, Bartkowska A, Jurči P, Przestacki D (2022) Influence of manufacturing parameters on microstructure, chemical composition, microhardness, corrosion and wear resistance of ZrC

24. coatings produced on Monel®400 using laser processing technology. Coatings 12:651. https://doi.org/10.3390/coatings12050651

24. Zhang Q, He J, Liu W, Zhong M (2003) Microstructure characteristics of ZrC-reinforced composite coating produced by laser cladding. Surf Coat Technol 162:140–146. https://doi.org/10.1016/S0257-8972(02)00697-7

25. Jiang M, Oikawa K, Ikeshoji T, Wulff L, Ishida K (2001) Thermodynamic calculations of Fe-Zr and Fe-Zr-C systems. J Phase Equilib 22:406–417

26. Bozzi AC, Biasoli de Mello JD (1999) Wear resistance and wear mechanisms of WC–12%Co thermal sprayed coatings in three-body abrasion. Wear 233–235:575–587. https://doi.org/10.1016/S0043-1648(99)00206-9

27. Yang Z, Jian Y, Chen Z, Qi H, Huang Z, Huang G, Xing J (2022) Microstructure, hardness and slurry erosion-wear behaviors of high-speed laser cladding Stellite 6 coatings prepared by the inside-beam powder feeding method. J Market Res 19:2596–2610. https://doi.org/10.1016/j.jmrt.2022.06.025

Publisher's note Springer Nature remains neutral with regard to jurisdictional claims in published maps and institutional affiliations.